Enhancing near-infrared avalanche photodiode performance by femtosecond laser microstructuring

Richard A. Myers, Richard Farrell, Arieh M. Karger, James E. Carey, and Eric Mazur

A processing technique using femtosecond laser pulses to microstructure the surface of a silicon avalanche photodiode (APD) has been used to enhance its near-infrared (near-IR) response. Experiments were performed on a series of APDs and APD arrays using various structuring parameters and post-structuring annealing sequences. Following thermal annealing, we were able to fabricate APD arrays with quantum efficiencies as high as 58% at 1064 nm without degradation of their noise or gain performance. Experimental results provided evidence to suggest that the improvement in charge collection is a result of increased absorption in the near-IR. © 2006 Optical Society of America

OCIS codes: 040.1240, 040.5170, 040.3060.

1. Introduction

There is a wide range of interest in improving the responsivity of silicon detectors in the near-infrared (near-IR) region of the electromagnetic spectrum. This interest is driven by the prevailing use of silicon throughout the semiconductor industries. However, while the use of silicon detectors is popular for optoelectronic applications, their use in the telecommunications industry is limited because the bandgap of ordinary bulk silicon is 1.12 eV.[1] This reduces the absorption and thus the photoresponse of silicon-based photodiodes at wavelengths beyond 1100 nm. While the maturity of high-power lasers near this bandgap makes them attractive for the development of rugged, long-range applications including free-space optical communications and laser radar, the responsivity of the silicon detectors to these wavelengths often fails to meet users' needs. Detectors with a higher responsivity in this range would help meet eye-safety requirements, allow a more compact package by reducing the laser power demands, and provide the sensitivity needed for many ranging or communication applications.[2–5]

R. A. Myers (rmyers@rmdinc.com), R. Farrell, and A. M. Karger are with Radiation Monitoring Devices, Inc., 44 Hunt Street, Watertown, Massachusetts 02472-4699. J. E. Carey and E. Mazur (Mazur@physics.harvard.edu) are with the Department of Physics and Division of Engineering and Applied Science, 9 Oxford Street, Cambridge, Massachusetts 02138.

Received 20 June 2006; accepted 30 June 2006; posted 7 August 2006 (Doc. ID 72082).

0003-6935/06/358825-07$15.00/0

© 2006 Optical Society of America

To achieve an enhanced near-IR response, fabrication of thick silicon photodiodes, including avalanche photodiodes (APDs) with internal gain, can compensate for the longer penetration depth of the radiation.[6] However, as the volume of bulk material increases, the detector noise also increases limiting the advantage of a thicker detector. Reflective surfaces on the backside of the detector have also been fabricated with varying degrees of success but with increased processing challenges.[7] Optical antireflection coatings can also improve the overall response, but the best commercial detectors using one or more of these techniques still does not achieve quantum efficiencies above 40% at the popular laser wavelength of 1064 nm. While other semiconductor materials, including indium gallium arsenide and germanium are used for near-IR detection, their higher noise characteristics, poor integration with existing silicon-based electronics, and higher material cost have sustained the desire for improved responsivity in silicon.[8,9]

Over the past several years, researchers have advanced the development of a surface structuring technique to enhance the absorption of radiation both below and above the bandgap of silicon.[10–13] Through the use of femtosecond or nanosecond lasers to form microstructures along the exposed silicon surface, absorption of silicon can be as high as 90% at wavelengths ranging from 250 to 2500 nm.[14] Further demonstrations of the absorption properties of bulk silicon and the effect of the laser microstructuring parameters have been reported in the literature.[15–18] Developmental work includes using the laser microstructuring to form a photodiode junction in an n-type

Samsung Exhibit 1011, Page 1 of 7

silicon wafer providing sensitivity to wavelengths up to 1600 nm.[19]

In this paper, we report the laser microstructuring of a silicon-based APD and APD arrays. Using a series of poststructuring fabrication steps including annealing, we have demonstrated responsivities two to three times greater than the unstructured APDs at near-IR wavelengths without degradation of other performance characteristics.

2. Experimental Methods

We fabricate our APDs from *n*-type neutron-transmutation-doped silicon wafers (30 Ω cm, 100-crystal orientation). Grooves are cut in the wafer with a diamond saw to define and isolate the individual pixel elements. This is followed by very deep boron diffusion in a high-temperature diffusion furnace. Polishing and chemical etching steps are then used to achieve the desired thickness of the drift and the *n*-type layers. The final structure is ~250 μm thick with a *p*–*n* junction 50 to 60 μm below the device surface.[20,21] To achieve high APD gain, a reverse bias is applied, expanding the width of the depletion region toward the silicon anode surface. As the depletion region width reaches toward the detector anode surface boundary, charges from defect states near the surface have a greater probability of being collected. Radiation Monitoring Devices, Inc.'s APDs have been carefully fabricated to achieve the highest gain without significantly increasing the leakage current until breakdown is reached.[22]

The laser microstructuring was done in vacuum using a Ti:sapphire laser at a wavelength of 800 nm, a pulse width of 100 fs, and a repetition rate of 1 kHz. The irradiating beam was directed normal to the anode side of the APD wafer, which was translated to allow for the structuring of a surface area larger than the focal spot size of 150 μm. The translation speed was adjusted so that the surface was exposed to an average of 10–400 laser pulses per unit area. To further evaluate the microstructuring process parameters, we also varied the laser fluence from 3 to 8 kJ/m^2 (average energy of 53–140 μJ). Formation of microstructures took place in atmospheres of SF_6, H_2S, N_2, and air at a constant background pressure of 500 Torr.

The microstructuring process removes silicon from the surface of the wafer, creating numerous defect sites and modifying the thickness of the APD surface layers. Because this process had to take place after the APD structures were produced, we attempted to minimize the volume of silicon removed to maintain the high-gain performance of the APD and limit any increase in the leakage current from the surface change collection. Both APD arrays and single element APDs with an active area of 2 mm × 2 mm were used throughout these studies.

Following texturing, the APD wafers were either packaged according to our standard processing techniques, or they underwent thermal annealing in a laboratory oven in a N_2 atmosphere. Annealing ranged from 400 to 1223 K for up to 24 h. Our standard packaging consists of coating the APD with a passivation layer, attaching electrical contacts to both the anode and cathode, mounting on a supporting substrate, and applying a polymer underfill. Two 16-element detector arrays that were microstructured are shown in Fig. 1. The effect of the microstructuring was evaluated across the array grooves and on individual pixels. One of the samples shown was divided into four different processing regions, each structured with a different number of laser pulses per unit area (0, 10, 100, and 300). The darkest region represents a greater number of laser pulses, while the shiny areas are unstructured APD pixels that were used for comparison.

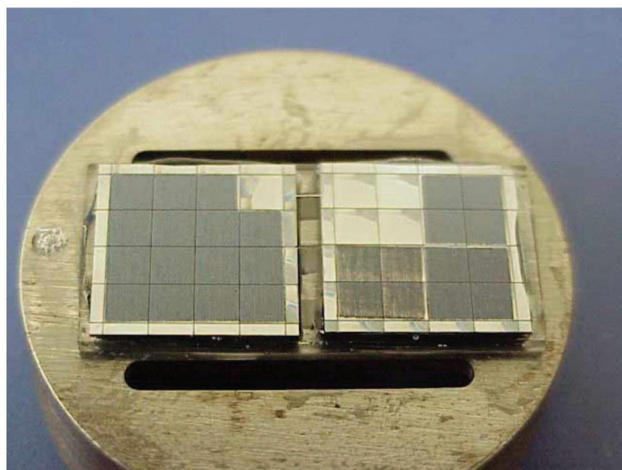

Fig. 1. (Color online) Picture of two microstructured APD arrays prior to packaging. Structuring was performed with an 800 nm fs laser operating at a fluence of 3.5 kJ/m^2 in an atmosphere of SF_6. The array on the right had four different structured regions with a pulse number ranging from 0 to 300. The shiny area is the bare silicon.

We investigated the effects of the processing conditions and thermal annealing on the performance of the APD detectors. Using radiation from a range of wavelengths emitted from a white-light source dispersed through a monochromator, we measured the photocurrent generated by each microstructured and unstructured APD. A 200 V bias was applied to each detector to ensure proper charge collection without internal gain. A National Institute of Standards and Technology (NIST) traceable photodiode was used to calibrate the absolute response of the detector. In addition, a reference photodiode was used to monitor the output of the white-light source over time.

The gain profile of both structured and nonstructured APDs was measured by employing a low-power, pulsed, or cw diode laser source. When recording the cw signal, a picoammeter (Keithley model 619) was used to monitor the APD output with no additional amplification electronics. The pulsed setup used a 1 μs laser pulse, a charge-sensitive amplifier (Cremat model CR-110), and a spectroscopy amplifier (Canberra model 2020) was used to amplify the APD output. The minimum detectable energy was measured with the

Samsung Exhibit 1011, Page 2 of 7

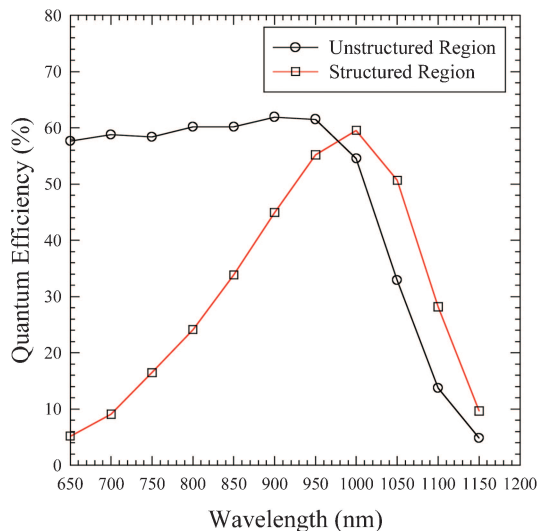

Fig. 2. (Color online) Quantum efficiency versus wavelength for a single-element APD that was partially microstructured. The structured region shows an enhanced signal in the near-IR but reduced responsivity below 950 nm. Data were recorded with a 200 V bias applied to the APD.

bias set to unity gain. The bias was then increased, and the photoinduced signal and the dark current were recorded at each setting. Neutral density filters were used to reduce the laser power as necessary. Response to radiation from 635 and 1060 nm laser diodes was evaluated.

A passively Q-switched microchip laser (Uniphase model NG-10120-101) with output radiation at 1064 and 532 nm was used to estimate the bandwidth of the detector with and without microstructuring. The pulse width of the laser was monitored with a 1 GHz photodiode and compared to the APD output at various bias settings.

To help evaluate whether the bandgap of silicon was altered following the microstructuring, the photocurrent generated from the detector was measured as a function of temperature. The devices were placed inside an aluminum enclosure that had optical and electrical feedthroughs. The enclosure was then placed in a heavily insulated liquid-nitrogen bath for cooling below 100 K, while a constant source of illumination at 1060 or 635 nm was incident upon the detectors. As the detector slowly warmed (<1 K/min) to room temperature, the unity-gain response at a reverse bias of 200 V was recorded. The responses from microstructured and unstructured APDs were compared.

3. Experimental Results

Figure 2 shows the quantum efficiency of a single element APD with structured and unstructured regions as a function of the wavelength. The data were collected with a 200 V bias across the APD junction to assist with the charge collection and ensure unity-gain response. Following the microstructuring, the response at wavelengths below 950 nm is dramatically reduced, while that at near-IR wavelengths is enhanced. The response at energies below the bandgap was enhanced by as much as a factor of 10, but the overall quantum efficiency was always relatively small (less than 0.01% at 1300 nm). These results were fairly consistent for most processing conditions.

Table 1 provides the values for the measured quantum efficiency (QE) at 1064 nm for several microstructured APD arrays or APD pixels as a function of various processing parameters. The equivalent unstructured devices exhibited a range of efficiencies that varied depending on the APD fabrication properties. The initial efficiencies following microstructuring were typically no more than 30% higher than the unstructured samples. However, the addition of a thermal annealing step increased the QE by more than a factor of 2. Consistent QE values at 1064 nm reached 40% or higher with low-temperature annealing and as high as 58% with high-temperature annealing. Thermal annealing did not affect the QE of the unstructured APDs that were used as a reference.

Table 1. Effect of Processing Conditions on the QE at 1064 nm

APD Sample	Laser Pulses	Laser Fluence (kJ/m^2)	Gas	QE before Annealing (Percentage at 1064 nm)	Annealing Temperature (K)/Time (h)	QE after Annealing (Percentage at 1064 nm)	Signal Ratio after/before Annealing
1	0	0	SF_6	25	1173/4	25	1
2	200	5	SF_6	15	673/2	34	2.3
3	200	5	SF_6	18	673/5	36	2.0
4	10	3.5	SF_6	28	673/2	41	1.5
5	100	3.5	SF_6	19	673/2	38	2.0
6	200	3.5	SF_6	21	673/2	38	1.8
7	400	3.5	SF_6	25	673/2	41	1.6
8	400	3.5	H_2S	27	673/3	42	1.6
9	200	3.5	Air	29	673/2	34	1.2
10	200	3.5	N_2	37	673/2	40	1.2
11	100	3.5	SF_6	NA[a]	1123/1[b]	48	NA[a]
12	100	3.5	SF_6	NA[a]	1173/1[b]	58	NA[a]
13	100	3.5	SF_6	NA[a]	1223/1[b]	54	NA[a]

[a]NA stands for not available.
[b]A p^+ dopant was applied to the surface before annealing.

Samsung Exhibit 1011, Page 3 of 7

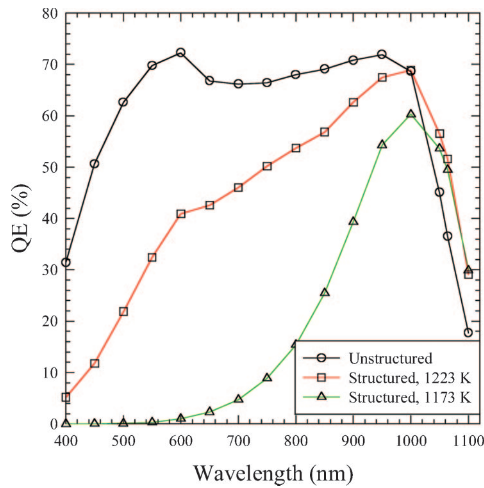

Fig. 3. (Color online) QE versus wavelength for an unstructured APD and two APDs annealed at high temperatures. The thermal annealing further enhances the near-IR response, while annealing at ~1173 K results in the improved response in the visible spectrum.

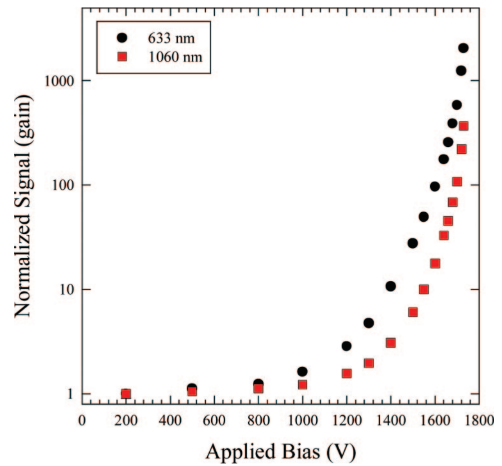

Fig. 4. (Color online) APD gain as a function of the applied bias for structured APD pixels. The gain dependence on the bias was nearly identical to the unstructured APDs for both 632 and 1060 nm.

We found that the most reliable microstructure processing used an average of 100 laser pulses at 62 μJ (3.5 kJ/m^2) in an atmosphere of SF_6. While the processing atmosphere did not appear to affect the QE prior to annealing, the relative increase following annealing was greater for devices that were structured in atmospheres of SF_6 or H_2S.[23] Increased laser fluence or a greater number of laser pulses per unit area were more damaging to the samples and did not lead to improved QEs, while fewer laser pulses and a lower fluence resulted in poor uniformity across the detector surface. Finally, microstructuring across the grooves between APD pixels did not produce a detrimental effect or limit the yield of functioning detectors. This promoted a means to structure an entire silicon wafer without limiting the existing planar processing capabilities.

The thermal annealing was considered essential to obtaining the enhanced near-IR response. The high temperatures (more than 1123 K) also allowed us to drive in an additional surface doping to assist charge collection. In addition to the enhancement in the near-IR, high-temperature thermal annealing improved the response in the visible spectrum. Figure 3 compares the response as a function of wavelength for a structured APD detector that was annealed at 1223 K with one that was annealed at 1173 K. Although we had limited sample numbers, the yield of devices that maintained their low noise performance appeared to decrease following the annealing at temperatures above 1173 K.

The amount of light transmitted and reflected from the silicon at normal incidence was characterized with an unpackaged, partially structured APD wafer that was annealed at 1173 K. Using a 1060 nm light source, we found that the unstructured silicon region had a transmission and a reflection of 42% and 33%, respectively. These values are consistent with our APD thickness of 250 μm. The structured region, on the other hand, had a transmission ranging from 4% to 7% and a reflection of less than 3%, indicating that up to 50% of the electrons created during absorption are not collected at the electrode.

APD gain and noise were measured prior to and following the microstructuring. Figure 4 shows the typical gain response curves as a function of bias for a microstructured APD at two different wavelengths. The maximum gain at 1060 nm approached 400, while the gain at 635 nm was larger than 1000. Interestingly, the gain and dark current dependence on the bias were nearly identical to the detectors that were not microstructured.

Figure 5 shows the response of a microstructured and unstructured APD to subnanosecond laser pulses at 532 and 1064 nm. The output from the APD was terminated with 50 Ω at an oscilloscope to collect the data. No additional amplification electronics were used during this measurement. There was very little difference in the speed of response of the two detectors with a slightly faster fall time measured from the microstructured detector. While the response of each detector was faster at the higher bias, the difference did not change.

The unity-gain response of a structured and unstructured APD was also compared as a function of temperature. Figure 6 shows the output signals normalized (to laboratory ambient) as a function of temperature. The decrease in QE as a function of temperature is expected, because the bandgap energy increases with decreasing temperature.[1] The bandgap of silicon ranges from 1.12 eV (1120 nm) at 300 K to 1.16 eV (1070 nm) at 50 K. Again, there was a negligible difference between the microstructured and unstructured APD response as a function of temperature. A similar performance also holds at 635 nm, where the QE for wavelengths far from the bandgap remains nearly constant with decreasing temperature.

Samsung Exhibit 1011, Page 4 of 7

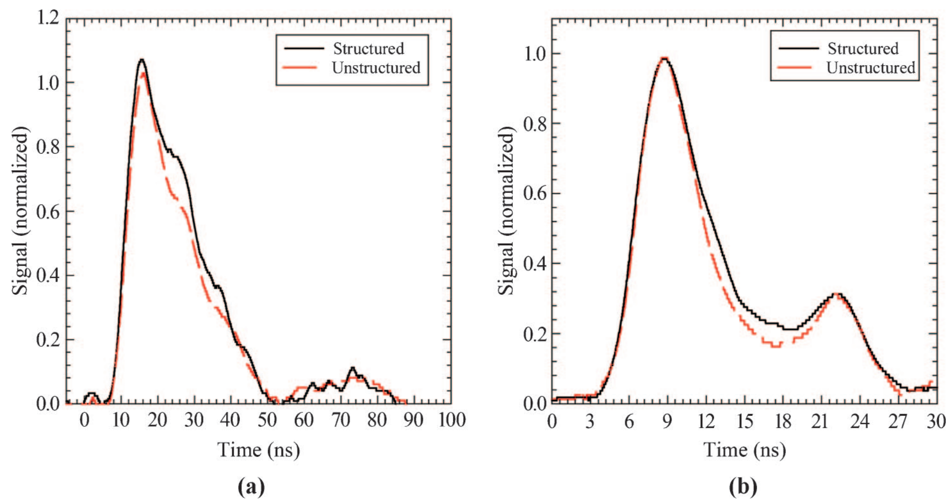

Fig. 5. (Color online) Response of a microstructured and unstructured APD to a subnanosecond pulse of radiation at (a) 532 nm and (b) 1064 nm. The response of the structured APD was nearly identical to the unstructured detector at all the tested bias settings. No amplification electronics were used in this measurement.

4. Discussion

The most significant result of this work was the ability to fabricate a silicon-based APD with a QE of 58% at 1064 nm. With usable gains of 400 to 500, this translates to a responsivity greater than 200 A/W. Equally important is the ability to integrate the microstructuring into a planar processing sequence without requiring additional labor-intensive steps.

Microstructuring in atmospheres of SF_6 or H_2S followed by thermal annealing produced an improvement in the QE for every APD detector tested. Previous observations showed that irradiation of silicon with femtosecond laser pulses in a sulfur atmosphere resulted in a high concentration of sulfur (~1%) in the disordered surface layer.[13,23] It is theorized that those sulfur atoms play a critical role in producing new energy states for absorption below bandgap absorption.[24] However, based on the measurements at 1300 nm in this study, it is apparent that the enhanced IR absorption does not result in an improved detector responsivity, suggesting that recombination through charge trapping hinders collection. In addition, the significant decrease in the QE for wavelengths below 950 nm also suggests that charges generated near the detector surface become trapped. Charges generated from photons at longer wavelengths, and thus absorbed deeper in the silicon, have a higher probability of being collected.

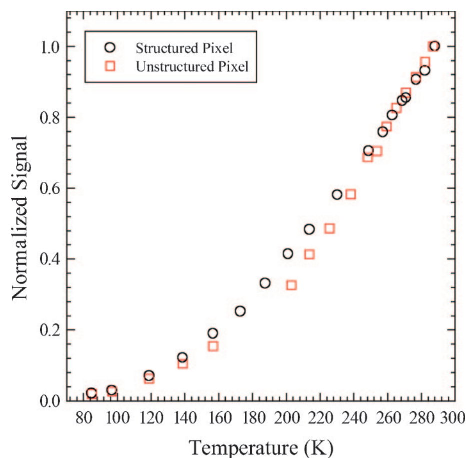

Fig. 6. (Color online) APD signal strength due to 1060 nm illumination as a function of temperature. The unity-gain signal (200 V bias) was recorded as the detector warmed from ~100 K. Both the microstructured and unstructured detectors had a similar dependence.

APDs structured in each background gas tested produced some enhancement in their QE prior to annealing, but only those processed in a sulfur-containing atmosphere exhibited a significant increase following the annealing. This suggests that the microstructuring alone produced a slight advantage for the longer-wavelength light, because surface scattering or photon trapping increases the effective path length through the structured APD compared with an unstructured detector. However, a second mechanism is needed to alter the dynamics of the trapping sites following thermal annealing. This secondary mechanism appears to be related to the sulfur content and annealing temperature. As the sample is thermally annealed, the charge collection increases, although previous studies have shown that the total absorption decreases.[14] Simple reorganization of defect sites reducing the trapping of electrons in the APD drift region is the most likely mechanism. Another possibility is an n-type silicon layer, which, research has shown, forms in the presence of a sulfur atmosphere during microstructuring.[19] This induced doping will create a near-surface p–n junction on our APDs, decreasing the ability for the charges to reach the collection electrode. We suspect that the high-temperature annealing may modify this layer and help compensate for this interference. However, further studies are required to validate this theory.

The detection of radiation with a long penetration depth is limited by lower achievable APD gains, be-

cause some of the radiation is absorbed in the depletion region of the detector, limiting its path length through the amplification region. Shorter wavelengths, on the other hand, are absorbed closer to the surface of the detector and achieve higher gain. This gain reduction was also observed in the structured detectors (Fig. 4). If the enhancement was strictly due to greater absorption near the surface region of the detector, we would have expected to measure a modification to the gain profile, including a larger maximum gain at 1060 nm. Because the gain dependence for the structured and unstructured APDs was nearly identical, we assumed that the photons detected are absorbed at nearly identical depths. This suggests that we are not taking advantage of the increased photon density absorbed near the APD surface.

The dramatic decrease in signal at wavelengths below 950 nm indicates that near-surface absorption of photons creates charges that are retrapped and not collected at the detector cathode. In addition, if the microstructured APD's enhancement was due to an increased amount of absorption near the surface region, we would have expected similar response speeds owing to the 1064 and 532 nm radiation following the microstructuring. However, the unchanged response and gain suggests that, unlike those created near the surface, the charge carriers are not slowed by the need to cross through the drift region prior to amplification. This lack of charge collection from the surface indicates that the microstructured layer functions as an antireflection coating increasing the total number of photons available for absorption but retrapping those charges created in the near-surface layer.

The experimental evidence also suggests that we are not taking advantage of new energy states created below the bandgap of pure silicon. This is observed through the detection of radiation near the silicon bandgap energy and the resulting decrease in the QE as a function of temperature (Fig. 6). This decrease was consistent for both microstructured and unstructured APD detectors despite the fact that half of the signal from the microstructured detector resulted from the microstructuring process. If the near-IR enhancement was caused by absorption into new energy states, we would have expected a greater difference in the temperature dependence, because the energy states would be lower than 1.1 eV. The lack of significant improvement in the detection of 1.3 μm radiation is consistent with the idea that charges created due to photoabsorption at new lower-energy states are not being collected.

Although further studies are required to fully explain some of the experimental results, it is apparent that the increased absorption results in an increase in the number of charge carriers. The large number of defect sites created by the microstructuring limits the flow of charges from the near-surface region. Thermal annealing reduces or alters some of the sulfur-induced charge-trapping sites or limits the effect of a competing n-type layer formed following the structuring.

5. Conclusion

Microstructuring of the surface layer of an APD with a femtosecond laser in an atmosphere of SF_6 has been shown to increase its responsivity in the near-IR to over 200 A/W at 1064 nm without increasing the leakage current or slowing its speed of response. An additional annealing step is required following the microstructuring to achieve these high responsivities. We have demonstrated this processing on the wafer scale without adding significant labor-intensive steps. Reduction in the QE at wavelengths below 900 nm may be alleviated with additional high-temperature annealing.

Comparisons of the responsivity from APD detectors that were microstructured and annealed under varying conditions have suggested a mechanism leading to the enhanced response in the near-IR. By monitoring the response of APD detectors microstructured in different background gases, we found that those processed in the presence of sulfur achieved the highest possible QE following annealing. Studies of the temperature and long-wavelength dependence of the responsivity suggest that the enhanced APD signal is a result of improved absorption in the silicon but is not related to additional energy bands created during the microstructuring. In addition, while the total absorption is increased, temporal bandwidth experiments and the observed decrease in detector response to short-wavelength radiation indicate that most of the charges collected result from absorption events occurring deeper than the near-surface, microstructured region. Further studies are required to answer some of the remaining questions about the mechanism and to determine its long-term stability.

The authors acknowledge the support of the National Aeronautic and Space Administration (contracts NAS302187 and NNGO4CA27C) for the research reported in this paper.

References

1. S. M. Sze, *Physics of Semiconductor Devices,* 2nd ed. (Wiley-Interscience, 1981).
2. L. T. Canham, T. I. Cox, A. Loni, and A. J. Simons, "Progress towards silicon optoelectronics using porous silicon technology," Appl. Surf. Sci. **102,** 436–441 (1996).
3. M. Okamura and S. Suzuki, "Infrared photodetection using a A-Si-H photodiode," IEEE Photon. Technol. Lett. **6,** 412–414 (1994).
4. M.-K. Lee, C.-H. Chu, Y.-H. Wang, and S. M. Sze, "1.55-mm and infrared-band photoresponsivity of a Schottky barrier porous silicon photodetector," Opt. Lett. **26,** 160–162 (2001).
5. M. Ghioni, A. Lacaita, G. Ripamonti, and S. Cova, "All-silicon photodiode sensitive at 1.3 micron with picosecond time resolution," IEEE J. Quantum Electron. **28,** 2678–2681 (1992).
6. R. Farrell, R. H. Redus, J. S. Gordon, and P. Gothoskar, "High gain APD array for photon detection," in *Photodetectors and Power Meters II,* K. Muray and K. J. Kaufmann, eds., Proc. SPIE **2550,** 266–273 (1995).
7. M. K. Emsley, O. Dosunmu, and M. S. Ünlü, "High-speed resonant-cavity enhanced silicon photodetectors on reflecting silicon-on-insulator substrates," IEEE Photon. Technol. Lett. **14,** 519–521 (2002).
8. A. Y. Loudon, P. A. Hiskett, G. S. Buller, R. T. Carline,

Samsung Exhibit 1011, Page 6 of 7

D. C. Herbert, W. Y. Leong, and J. G. Rarity, “Enhancement of the infrared detection efficiency of silicon photon-counting avalanche photodiodes by use of silicon germanium absorbing layers,” Opt. Lett. **27,** 219–221 (2002).
9. S.-B. Ko and H. T. Henderson, “The use of multiple internal reflection on extrinsic silicon infrared detection,” IEEE Trans. Electron. Devices **ED-27,** 62–65 (1980).
10. T.-H. Her, R. J. Finlay, C. Wu, S. Deliwala, and E. Mazur, “Microstructuring of silicon with femtosecond laser pulses,” Appl. Phys. Lett. **73,** 1673–1675 (1998).
11. C. Wu, C. H. Crouch, L. Zhao, J. E. Carey, R. Younkin, J. A. Levinson, E. Mazur, R. M. Farrell, P. Gothoskar, and A. Karger, “Near-unity below-band-gap absorption by microstructured silicon,” Appl. Phys. Lett. **78,** 1850–1852 (2001).
12. R. Younkin, J. E. Carey, E. Mazur, J. A. Levinson, and C. M. Friend, “Infrared absorption by conical silicon microstructures made in a variety of background gases using femtosecond-laser pulses,” J. Appl. Phys. **93,** 2626–2629 (2003).
13. C. H. Crouch, J. E. Carey, M. Shen, E. Mazur, and F. Y. Génin, “Infrared absorption by sulfur-doped silicon formed by femtosecond laser irradiation,” Appl. Phys. A **79,** 1635–1641 (2004).
14. C. H. Crouch, J. E. Carey, J. M. Warrender, M. J. Aziz, E. Mazur, and F. Y. Génin, “Comparison of structure and properties of femtosecond and nanosecond laser-structured silicon,” Appl. Phys. Lett. **84,** 1850–1852 (2004).
15. A. J. Pedraza, J. D. Fowlkes, and D. H. Lowndes, “Silicon microcolumn arrays grown by nanosecond pulsed-eximer laser irradiation,” Appl. Phys. Lett. **74,** 2322–2324 (1999).
16. J. T. Zhu, Y. F. Shen, W. Li, X. Chen, G. Yin, D. Y. Chen, and Z. Li, “Effects of polarization on femtosecond laser pulses structuring silicon surfaces,” Appl. Surf. Sci. **252,** 2752–2756 (2006).
17. J. T. Zhu, G. Yin, M. Zhao, D. Y. Chen, and L. Zhao, “Evolution of silicon surface microstructures by picosecond and femtosecond laser irradiations,” Appl. Surf. Sci. **245,** 102–108 (2005).
18. J. Bonse, K. W. Brzezinka, and A. J. Meixner, “Modifying single-crystalline silicon by femtosecond laser pulses: an analysis by microraman spectroscopy, scanning laser microscopy and atomic force microscopy,” Appl. Surf. Sci. **221,** 215–230 (2004).
19. J. E. Carey, C. H. Crouch, M. Shen, and E. Mazur, “Visible and near-infrared responsivity of femtosecond-laser microstructured silicon photodiodes,” Opt. Lett. **30,** 1773–1775 (2005).
20. R. Farrell, K. Vanderpuye, L. Cirignano, M. R. Squillante, and G. Entine, “Radiation detection performance of very high gain avalanche photodiodes,” Nucl. Instrum. Methods A **353,** 176–179 (1994).
21. R. Redus and R. Farrell, “Gain and noise in very high gain avalanche photodiodes: theory and experiment,” in *Hard X-Ray/Gamma Ray and Neutron Optic Sensors and Applications,* R. B. Hoover and F. P. Doty, eds., Proc. SPIE **2859,** 288–297 (1996).
22. R. Farrell, K. Shah, K. Vanderpuye, R. Grazioso, R. Myers, and G. Entine, “APD arrays and large area APDs via a new planar processing,” Nucl. Instrum. Methods. A **442,** 171–178 (2000).
23. M. A. Sheehy, L. Winston, J. E. Carey, C. M. Friend, and E. Mazur, “Role of the background gas in the morphology and optical properties of laser-microstructured silicon,” Chem. Mater. **17,** 3583–3586 (2005).
24. E. Janzén, R. Stedman, G. Grossman, and H. G. Grimmeiss, “High-resolution studies of sulfur- and selenium-related donor center in silicon,” Phys. Rev. B **29,** 1907–1918 (1984).

Samsung Exhibit 1011, Page 7 of 7